Iron-containing MCM-41 catalysts for Baeyer–Villiger oxidation of ketones using molecular oxygen and benzaldehyde

Tomonori Kawabata [a], Yoshihiko Ohishi [a], Satoko Itsuki [a], Naoko Fujisaki [a],
Tetsuya Shishido [b], Ken Takaki [a], Qinghong Zhang [c], Ye Wang [c], Katsuomi Takehira [a,*]

[a] Department of Chemistry and Chemical Engineering, Graduate School of Engineering, Hiroshima University, Kagamiyama 1-4-1,
Higashi-Hiroshima 739-8527, Japan
[b] Department of Chemistry, Tokyo Gakugei University, Nukui-kita 4-1-1, Koganei, Tokyo 184-8501, Japan
[c] State Key Laboratory for Physical Chemistry of Solid Surfaces, Department of Chemistry, Xiamen University, Xiamen 361005, China

Abstract

Iron(III)-containing mesoporous silica (MCM-41) with Fe contents up to 1.8 wt% have been prepared by direct hydrothermal synthesis (DHT) and template ion exchange (TIE) methods. Characterizations of these catalysts have been done by XRD, XPS, diffuse reflectance UV–vis, ESR, Mössbauer, and XAFS spectroscopies. Fe species in MCM-41 materials are tetrahedrally coordinated for the DHT method with Fe contents up to 1.1 wt% while those are mainly octahedrally coordinated for the TIE method. Among these catalysts, ferrisilicate and Fe_2O_3/Cab-O-Sil as references, Fe-MCM-41-DHT exhibited the highest catalytic activity for Baeyer–Villiger (B–V) oxidation of ketones using molecular oxygen and benzaldehyde. The prominent performance of the Fe-MCM-41-DHT could be ascribed to both tetrahedrally coordinated Fe^{3+} incorporated inside the framework of MCM-41 and its uniform nano-order mesopores allowing the access of bulky compounds to the active sites. Furthermore, this heterogeneous Fe catalyst was reusable without any appreciable loss in activity and selectivity. It has been confirmed by IR spectroscopy that the Fe-MCM-41-DHT-catalyzed B–V reaction proceeded via coordination of carbonyl groups of ketone to Fe^{3+}.
© 2005 Elsevier B.V. All rights reserved.

Keywords: MCM-41; Baeyer–Villiger reaction; Iron; Heterogeneous catalyst; Benzaldehyde

1. Introduction

MCM-41 materials possess a periodic framework of regular mesopores with a considerably high surface area [1], and have attracted great attention as a support for creating novel heterogeneous catalysts [2]. A wide variety of metal ions can be readily introduced by the direct hydrothermal (DHT) and the template ion exchange (TIE) methods. Especially, by using the DHT methods, atomically isolated metal species can be substituted isomorphously for silicon atoms into the MCM-41 framework and act as catalytically active centers. Up to now, some transition metals of Ti [3–13], V [6,14–18], Cr [6,19–24], Fe [25,26], Cu [27], and have been successfully incorporated into MCM-41 skeletons, achieving high catalytic activity and selectivity for various types of oxidation reactions.

Baeyer–Villiger (B–V) oxidation of ketones is widely used for the synthesis of various lactones or esters. Various B–V reactions have been commonly carried out using peracid oxidants such as persulfuric acid, perbenzoic acid, *m*-chloroperbenzoic acid (*m*-CPBA), and hydrogen peroxide [28–32]. A combination of molecular oxygen and aldehydes under heterogeneous catalysis has also been extensively studied [33–38] since Kaneda et al. reported the oxidative cleavage of alkenes into carbonyl compounds over RuO_2–CH_3CHO–O_2 system [39]. These heterogeneous B–V reactions have the following advantages

_____
* Corresponding author. Tel.: +81 82 424 7744; fax: +81 82 424 7744.
  E-mail address: takehira@hiroshima-u.ac.jp (K. Takehira).

over the homogeneous catalysis: (1) simplicity in synthetic operations, (2) prevention of the production of salt wastes during neutralization of the catalysts or reagents, and (3) reusability of the solid catalyst [40–42]. The use of iron metal as catalytically active species is significantly attractive because the iron-containing compounds generally show low toxicity [43] and are easily available.

In the course of our studies on the syntheses of iron-containing MCM-41 catalysts by the DHT and TIE methods, we have found that two types of metal ion species could be created: small sized iron oxide clusters in the channel of MCM-41 for the TIE method, and tetrahedrally coordinated Fe^{3+} incorporated inside the framework of MCM-41 for the DHT method [26]. It has been found that Fe-MCM-41 prepared by the DHT method exhibited higher catalytic activity for the epoxidation of styrene with H_2O_2 than that by the TIE method [26]. In the present paper, we report the B–V reaction of ketones using the heterogeneous iron-containing MCM-41 catalysts. Various ketones readily reacted to afford the corresponding lactone compounds with a Fe-MCM-41-PhCHO-O_2 system at low reaction temperatures.

2. Experimental

2.1. Catalyst preparation

Fe-MCM-41 was prepared by both DHT and TIE methods. For the DHT procedure, aqueous sodium silicate solution (15.4 g: 55 wt% SiO_2), ferric nitrate, and hexadecyltrimethylammonium bromide (26.4 g) was dissolved in distilled water (80 mL) and pH was adjusted to 10.8 with 4 M HCl. The obtained gel was stirred for 1 h at room temperature, and then transferred to a Teflon bottle, which was placed in a stainless-steel autoclave. After hydrothermal synthesis at 150 °C for 48 h, the resultant solid was recovered by filtration, thoroughly washed with deionized water (20 L), and dried at 40 °C in vacuum for 24 h. Calcination of the dried sample at 550 °C in a flow of dry air (1 L min^{-1}) afforded the Fe-MCM-41-DHT as white powder. For the TIE synthesis of Fe-MCM-41, 2 g of the as-synthesized MCM-41 containing ca. 50 wt% of template cations was added to an ethanol solution of ferric nitrate (in 40 mL of H_2O). The mixture was stirred vigorously at room temperature for 1 h, and then kept at 80 °C for 20 h. The as-synthesized sample was calcined at 550 °C for 6 h in a flow of dry air (1 L min^{-1}) to give Fe-MCM-41-TIE as brown powder (Si/Fe = 79, Fe: 1.2 wt%).

Ferrisilicate with the MFI structure and Fe_2O_3/Cab-O-Sil were also prepared as control. Ferrisilicate was synthesized according to Ref. [44] by the hydrothermal method at 170 °C for 72 h using tetraethyl orthosilicate, ferric nitrate, and tetrapropylammonium hydroxide. The as-synthesized ferrisilicate was calcined by the same method as that for Fe-MCM-41. Fe_2O_3/Cab-O-Sil was obtained by a con-

ventional impregnation method using an aqueous solution of ferric nitrate and nonporous Cab-O-Sil (M5, Acros Organics).

2.2. Catalyst characterization

Inductively coupled plasma (ICP) optical emission spectroscopy was used for the determination of the metal content in each sample synthesized above. The measurements were performed with a Perkin-Elmer OPTIMA 3000. N_2-adsorption studies were carried out on a Belsorp 18SP equipment (volumetric), and all the samples were pretreated in vacuum at 200 °C for 12 h before the measurements. The pore-size distribution was evaluated from the adsorption isotherm by the Dollimore–Heal (DH) method [45]. X-ray diffraction (XRD) patterns were collected on an SRA M18XHF diffractometer (MAC Science Co. Ltd., Japan) with Cu Kα radiation (40 kV, 300 mA). The Fe K-edge X-ray absorption fine structure (XAFS) was measured at room temperature in a fluorescence mode at a beam line BL9A station of Photon Factory, at the High Energy Accelerator Research Organization (Tsukuba, Japan), operated at 2.5 GeV with about 350–380 mA of ring current. Details of data analysis followed the reported procedure [46]. The diffuse reflectance UV–vis spectroscopic measurements were recorded on a Perkin Elmer UV/VIS/NIR (Lambda 900) spectrometer. The spectra were collected at 200–700 nm referenced to $BaSO_4$. ESR spectra were measured at X-band (∼9 GHz) using a JEOL RE series JES-RE1X ESR spectrometer. The sample was placed in a quartz tube with an inner diameter of 3 mm and measured at room temperature. XPS measurements were performed on a Shimadzu ESCA-85 spectrometer working with a hemispherical analyzer. All binding energy values were referenced to C 1s (284.6 eV). Transmission Mössbauer spectra of pelletized powder samples were recorded at room temperature, using a constant acceleration mode (Topologic System Co.) of a radiation source with about 40 MBq ^{57}Co(Cr) and a YAP scintillation counter. Doppler velocity was calibrated with reference to α-Fe. Fourier transfer infrared spectroscopy (FT-IR) was recorded on a Shimadzu FTIR-8300 using a KBr disk method.

2.3. Catalytic testing

The Baeyer–Villiger oxidation of ketones was carried out using a batch-type reactor. In a typical reaction, 0.2 g of catalyst was added to a glass flask precharged with 2-adamantanone (1 mmol), benzaldehyde (3 mmol), and acetonitrile (10 mL). Oxygen (10 mL min^{-1}) was bubbled into the stirred solution. The heterogeneous reaction mixture was stirred at 25 °C for 15 h, and the catalyst was removed by filtration. The catalyst was washed with acetone, followed by drying at 110 °C and reused for the next reaction. The products in the filtrate were analyzed by GC (BPX-5, 30 M × 0.25 mm).

Table 1
Properties of various iron-containing catalysts

Sample[a]	Si/Fe in preparation gel	Si/Fe by ICP	Fe content (wt%)	Surface area $(m^2 \, g^-)^1$	Pore diameter (nm)	a_0[b] (nm)	Color of Sample	
							As-synthesized	Calcined
MCM-41	0	0	0	1043	2.7	4.37	White	White
Fe-MCM-41-DHT(200)	200	163	0.6	1043	2.7	4.39	White	White
Fe-MCM-41-DHT(100)	100	105	0.9	1173	3.0	4.60	White	White
Fe-MCM-41-DHT(75)	75	86	1.1	1078	3.0	4.70	White	White
Fe-MCM-41-DHT(50)	50	50	1.8	1016	3.0	4.66	White	Off white
Fe-MCM-41-TIE(102)	102	102	0.9	1220	2.7	4.37	Brown	Brown
Fe-MCM-41-TIE(75)	75	75	1.2	983	2.7	4.40	Brown	Brown
Fe$_2$O$_3$/Cab-O-Sil(96)	–	96	1.0	150	–	–	Brown	Brown
Ferrisilicate (MFI, 48)	–	48	1.9	350	0.55	–	White	White

[a] The numbers in parentheses are the Si/Fe atomic ratios.
[b] Unit cell parameter.

3. Results and discussion

3.1. Structure of the catalysts

The physicochemical properties of Fe-MCM-41 catalysts prepared by both DHT and TIE methods are shown in Table 1 together with those of Fe$_2$O$_3$/Cab-O-Sil(96) and ferrisilicate(48) (numbers in parentheses show the Si/Fe ratio determined by ICP). All the Fe-MCM-41 catalysts and Fe-free MCM-41 exhibited large surface area of 1000–1200 $m^2 \, g^{-1}$ and pore volume of 0.75–1.0 mL g^{-1}. Narrow pore distribution around 2.5–3.0 nm was observed with all the MCM-41 samples. XRD patterns of as-synthesized and Fe^{3+}-incorporated MCM-41 showed typical reflection lines of (1 0 0), (1 1 0), (2 0 0), and (2 1 0) in the range 2°–8°, characteristic of MCM-41 (Fig. 1). These results confirmed the retention of MCM-41 structure even after the introduction of iron species by both DHT and TIE methods. The surface areas of reference samples such as Fe$_2$O$_3$/Cab-O-Sil and fer-
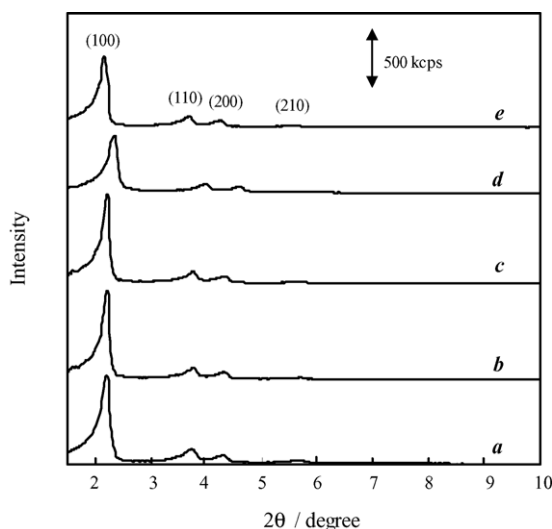

Fig. 1. XRD patterns of the Fe-MCM-41: (a) Fe-MCM-41-DHT(50), (b) Fe-MCM-41-DHT(75), (c) Fe-MCM-41-DHT(100), (d) Fe-MCM-41-TIE(75), and (e) Fe-MCM-41-TIE(102).

risilicate were 150 and 350 $m^2 \, g^{-1}$, respectively. The color of the Fe-containing samples synthesized in this work is a simple indication of whether bulk iron oxide exists [44]. All the as-synthesized Fe-MCM-41-DHT samples exhibited a white color, suggesting that no bulk iron oxide existed and all the iron cations were probably incorporated inside the framework after hydrothermal synthesis. The white color was kept after the calcination of the DHT samples with Fe contents lower than ca. 1.0 wt%. As the Fe content exceeded ca. 1.0 wt%, the calcined DHT sample became off-white in color, possibly suggesting the presence of the extraframework iron. On the other hand, the brown color of each TIE sample indicates that there exist aggregated iron oxide clusters as observed in Fe$_2$O$_3$/Cab-O-Sil(96).

Unit cell parameter (a_0) increased with the introduction of iron into MCM-41 by the DHT method up to the Fe content of ca. 1.0 wt% and then leveled off. This trend can be accounted for that Fe^{3+} cations are incorporated into the framework of MCM-41 to replace Si^{4+} and there exist an upper limit of iron content incorporated inside the framework. A similar expansion in parameter is observed by Bourlineos et al. [47] and Selvam et al. [48] for Fe^{3+} substituted MCM-41 samples. On the other hand, the a_0 values did not change significantly on introduction of iron into MCM-41 by the TIE method, suggesting that the substitution amount is very small during the TIE procedures.

Fig. 2 shows the diffuse reflectance UV–vis spectra. All DHT samples used in this work mainly exhibited a peak at ca. 265 nm as seen in a typical spectra of Fe-MCM-41-DHT(75) with iron contents of ca. 1.0 wt% (Fig. 2c), which was similar to that for ferrisilicate containing tetrahedrally coordinated iron species [26]. This band could be assigned to the $d\pi$–$p\pi$ charge transfer between the Fe and O atoms in the framework of Fe–O–Si in the zeolite [49]. The contribution of long wavelength to this band increased with increasing Fe content in the DHT sample, indicating the formation of extraframework iron or aggregated iron oxide clusters at high Fe content as seen for Fe-MCM-41-DHT(50) (Fig. 2a). These results further suggest that there exists an upper limit of iron content incorporated inside the framework of MCM-41. Ac-
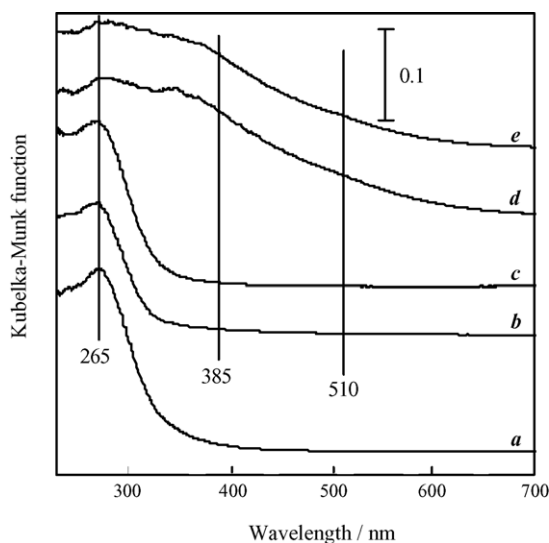
Fig. 2. Diffuse reflectance UV–vis spectra of Fe-MCM-41: (a) Fe-MCM-41-DHT(50), (b) Fe-MCM-41-DHT(75), (c) Fe-MCM-41-DHT(100), (d) Fe-MCM-41-TIE(75), and (e) Fe-MCM-41-TIE(102).

Table 2
XPS analysis of the Fe-MCM-41-DHT and TIE catalysts

Catalyst	Binding energy, E_b (eV)[a]		
	Fe 2p$^{3/2}$	Si 2p	O 1s
Fe-MCM-41 (DHT)	711.0	103.6	532.9
Fe-MCM-41 (TIE)	710.8	103.8	532.8

[a] Referenced to C 1s = 284.6 eV.

tually additional peaks were observed at long wavelength for the TIE samples possessing extraframework iron or aggregated iron oxide clusters (Fig. 2d and e). In addition to the peak at 265 nm, bands at ca. 385 and 510 nm appeared for the TIE samples, and both bands became stronger with increasing Fe content. These bands were also observed for Fe_2O_3/Cab-O-Sil, and the intensities were much enhanced compared to those of Fe-MCM-41-TIE(75), indicating that iron species mainly exist as iron oxide clusters outside framework of Cab-O-Sil.

According to the results of X-ray absorption spectroscopy [26], the authors concluded that iron atoms in ferrisilicate are in regular tetrahedral coordination, whereas those in α-Fe_2O_3 are mainly in distorted octahedral coordination since the preedge peak at ca. 7112 eV in the XANES spectra of

the catalysts, attributed to the so-called 1s–3d dipolar forbidden transition, the most strong for ferrisilicate and the most weak for α-Fe_2O_3. Moreover the framework of MCM-41 in Fe-MCM-41-DHT is essentially amorphous whereas that of ferrisilicate is crystalline judging from the peak intensity. The Si–O–Fe bonds sitting in the amorphous framework of Fe-MCM-41 prepared by the DHT method may thus be connected with more relaxing angles than those in ferrisilicate. Fe-MCM-41-TIE gave a smaller preedge peak compared to the DHT, followed by Fe_2O_3/Cab-O-Sil and α-Fe_2O_3, suggesting that iron in both Fe-MCM-41-TIE and Fe_2O_3/Cab-O-Sil was partly dispersed as the tetrahedrally coordinated species during the preparation.

The XPS binding energy data for Fe-MCM-41-DHT(75) and -TIE(75) catalysts are given in Table 2. Both TIE and DHT samples showed the binding energies of Fe 2p$^{3/2}$ at 711.0 eV, indicating that the Fe species are in a trivalent oxidation state [44]. Mössbauer spectra for Fe-MCM-41-DHT(75) and -TIE(75) are shown in Fig. 3, and the parameters determined by fitting the data are listed in Table 3. The doublet lines and Mössbauer parameters of both samples are indicative of high spin paramagnetic Fe^{3+} species in the MCM-41 material. It was reported that Fe^{3+} species give the isomer shift (IS) smaller than 0.3 mm s^{-1} in the tetrahedral coordination and that greater than 0.3 mm s^{-1} in the octahedral coordination [50]. On the other hand, Tuel et al. [51] recently reported that the value of IS in zeolites containing tetrahedral Fe can vary between 0.2 and 0.35 mm s^{-1}, de-
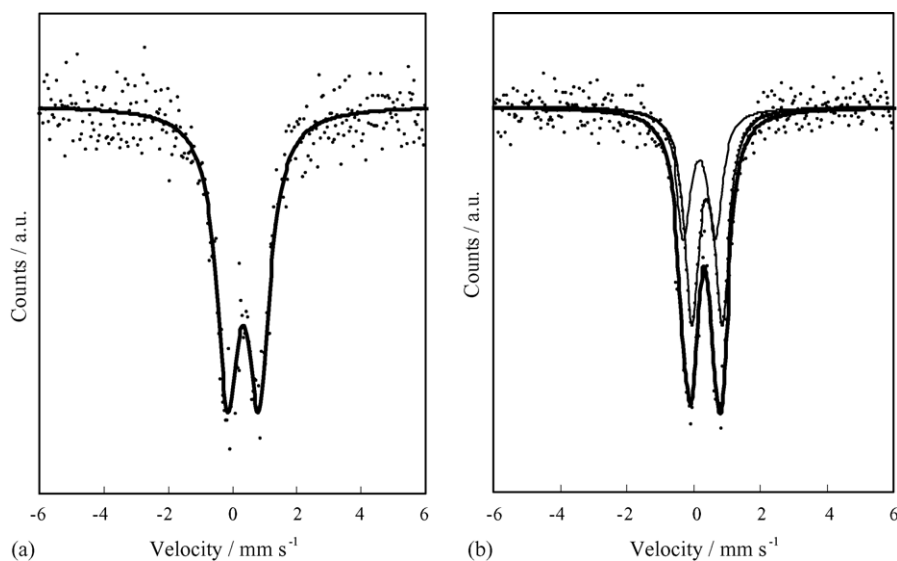

Fig. 3. Mössbauer spectra of: (a) Fe-MCM-41-DHT, and (b) Fe-MCM-41-TIE catalysts.

Table 3
Mössbauer parameters of the Fe-MCM-41 catalysts

Catalyst	Isomer shift, IS (mm s^{-1})	Quadrupole splitting, QS (mm s^{-1})	Line-width (mm s^{-1})	Spectral contribution (%)	
Fe-MCM-41 (DHT)	0.34	0.98	0.82	100	Tetrahedral Fe^{3+}
Fe-MCM-41 (TIE)	0.19	0.95	0.49	38	Tetrahedral Fe^{3+}
	0.41	0.91	0.49	62	α-Fe$_2$O$_3$

pending on the zeolite structure and the synthesis procedure. Such values were obtained on highly crystalline materials and thus cannot be directly extrapolated to amorphous systems. Considering the amorphous nature of the Fe-MCM-41-DHT shown by Fe K-edge XAFS experiments, it is assumed that a Fe^{3+} cation with a tetrahedral coordination environment was exclusively formed within the framework of Fe-MCM-41-DHT. Indeed, the broader line width (0.82 mm s^{-1}) compared to the Fe-incorporated silica (0.44–0.51 mm s^{-1}) reported by Tuel et al. [51] and the Fe-incorporated NaY zeolite (0.33–0.52 mm s^{-1}) by Fejes et al. [52] suggests that the iron cations in Fe-MCM-41-DHT are distributed in the sites with slightly different chemical environments with essentially relaxed angles of Si–O–Fe bonds. On the other hand, most of Fe^{3+} species existed as aggregated iron oxide clusters and a part of Fe^{3+} was incorporated into the tetrahedral sites on Fe-MCM-41-TIE. These are consistent with the results of UV–vis and Fe K-edge XAFS studies [26].

3.2. Oxidation of 2-adamantanone, etc.

The results of Baeyer–Villiger oxidations of 2-adaman-tanone (**1**) with various heterogeneous catalysts are summa-rized in Table 4. The activity of Fe-, Cu-, Ni-, and Mn-MCM-41-DHT for the B–V oxidation in acetonitrile solvent was tested. It is notable that the B–V oxidation hardly proceeded in the absence of the catalyst at 50 °C for 4 h (entry 15). Among the metals tested, Fe showed the highest activity. Cu-MCM-41-DHT also afforded **2** in a moderate yield (entry 9). The order of activity of Fe- and Cu-MCM-41 catalysts was in a marked contrast to Fe- and Cu-incorporated hydrotalcites (HT); i.e., Mg-Al-Cu-HT gave much higher yield of **2** than Mg-Al-Fe-HT for the B–V oxidation of **1** [36]. Neither Ni-nor Mn-MCM-41 afforded **2** (entries 10 and 11). When three equivalents of benzaldehyde with respect to 2-adamantanone was used in the presence of molecular oxygen, 4-oxatricyclo [4.3.1.13,8] undecan-5-one (**2**) was obtained together with benzoic acid. Use of molecular oxygen alone or H$_2$O$_2$ re-sulted in no production of oxygenated products. Among the solvents used, 1,2-dichloroethane afforded the highest yield of **2** (61%, entry 3) although the selectivity to **2** was low due to the formation of polymers. Acetonitrile was the secondary optimal solvent and gave **2** in 58% yield (entry 1), which is in contrast to the results obtained under the metal catalyst-free Baeyer–Villiger reactions [34], wherein acetonitrile was quite poor solvent. On the other hand, ethyl acetate, 1,4-dioxane,

Table 4
B–V reaction of 2-adamantanone (**1**) using various catalysts[a]
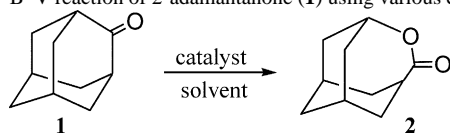
Entry	Catalyst	Solvent	Conversion (%)[b]	Yield (%)[b]
1	Fe-MCM-41 (DHT)	Acetonitrile	68	58
2	Fe-MCM-41 (TIE)	Acetonitrile	62	50
3	Fe-MCM-41 (DHT)	1,2-Dichloroethane	96	61
4	Fe-MCM-41 (DHT)	Ethyl acetate	7	6
5	Fe-MCM-41 (DHT)	1,4-Dioxane	2	1
6	Fe-MCM-41 (DHT)	DMF	0	0
7	Fe-MCM-41 (DHT)	Toluene	0	0
8	Fe-MCM-41 (DHT)	Ethanol	0	0
9	Cu-MCM-41 (DHT)	Acetonitrile	64	42
10	Ni-MCM-41 (DHT)	Acetonitrile	14	10
11	Mn-MCM-41 (DHT)	Acetonitrile	0	0
12	Fe$_2$O$_3$/Cab-O-Sil	Acetonitrile	49	27
13	ferrisilicate	Acetonitrile	30	17
14	Fe(NO$_3$)$_3$9H$_2$O	Acetonitrile	51	32
15	No	Acetonitrile	3	3

[a] Reaction conditions; catalyst (0.2 g, active metal species: 0.04 mmol), **1** (1 mmol), benzaldehyde (3 mmol), solvent (10 mL), O$_2$ (10 mL min^{-1}), 50 °C, 4 h.
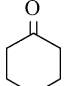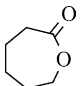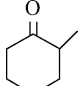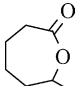[b] Determined by GC and calculated based on **1**.
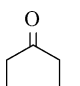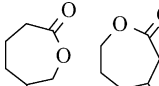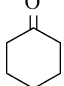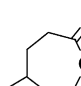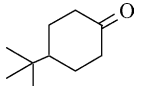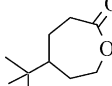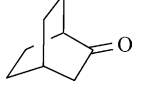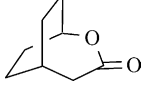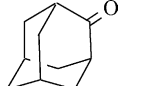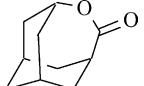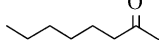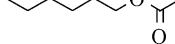
DMF, toluene, and ethanol showed unfavorable effects in this B–V oxidation.

Fe-MCM-41 synthesized by the DHT method exhibited higher catalytic activity than that by the TIE method (entries 1 and 2), as observed in the epoxidation of styrene with H_2O_2 [25]. 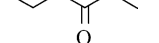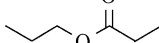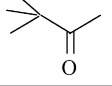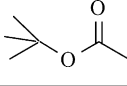It is likely that the tetrahedrally coordinated and atomically isolated iron sites are responsible for the B–V oxidation. Both conversion of **1** and selectivity to **2** of the Fe-MCM-41-DHT were greater than those of ferric nitrate, a precursor of the Fe-MCM-41 (entry 14). Moreover, Fe-MCM-41-DHT exhibited remarkably higher yield of **2** than Fe_2O_3/Cab-O-Sil and ferrisilicate (entries 1, 12, and 13). The local structure of iron species in Fe_2O_3/Cab-O-Sil resembles that in Fe-MCM-41-TIE; iron oxide clusters were formed on the silica support. In contrast, ferrisilicate possesses tetrahedral iron species surrounded by the oxygen atoms in the framework. Presumably,

small pore size (ca. 0.55 nm) of ferrisilicate obstruct an access of the bulky compound such as 2-adamantanone to their active sites. Thus, the high catalytic activity of the Fe-MCM-41-DHT can be ascribed to both tetrahedrally coordinated Fe^{3+} and its mesopores allowing the access of bulky compounds to active Fe sites.

The scope of substrates for the B–V reaction catalyzed by the Fe-MCM-41-DHT was examined and the typical results are shown in Table 5. The B–V reactions of various cyclic ketones occurred smoothly to afford selectively the corresponding lactones, even at room temperature. The Fe-MCM-41-DHT catalyst, however, was not active for the oxidation of acyclic aliphatic ketones and only small amounts of the desired esters were detected by GC. This behavior was also observed in copper or nickel-catalyzed homogeneous B–V reactions [53].

Table 5
Baeyer–Villiger oxidation of various ketones using Fe-MCM-41-DHT[a]

Entry	Ketone	Product	Conversion (%)[b]	Yield (%)[b]
1	(cyclohexanone)	(ε-caprolactone)	85	77
2	(2-methylcyclohexanone)	(lactone)	71	58
3	(3-methylcyclohexanone)	(lactones, 1:1)	65	62
4	(4-methylcyclohexanone)	(lactone)	79	75
5	(4-tert-butylcyclohexanone)	(lactone)	78	76
6	(bicyclic ketone)	(lactone)	87	77[c]
7	(2-adamantanone)	(lactone)	80	7
8	(acyclic ketone)	(ester)	0	No reaction
9	(acyclic ketone)	(ester)	Trace	Trace
10	(pinacolone)	(ester)	0	No reaction

[a] Fe-MCM-41-DHT (0.2 g, Fe: 0.04 mmol), ketone (1 mmol), MeCN (10 benzaldehyde (3 mmol), O_2 (l0 mL min^{-1}), 25 °C, 15 h.
[b] Determined by GC and calculated based on ketone.
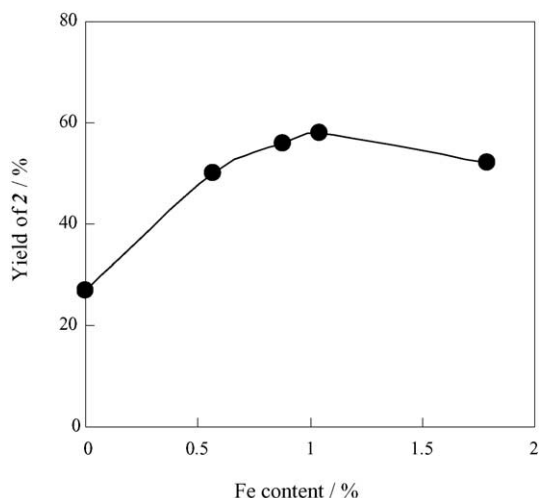[c] A small amount of isomer was detected.

Fig. 4. Effect of Fe content on B–V oxidation of 2-adamantanone. Fe-MCM-41-DHT (0.2 g), MeCN (10 mL), 2-adamantanone (1 mmol), benzaldehyde (3 mmol), O_2 (10 mL min^{-1}), 50 °C, 4 h.
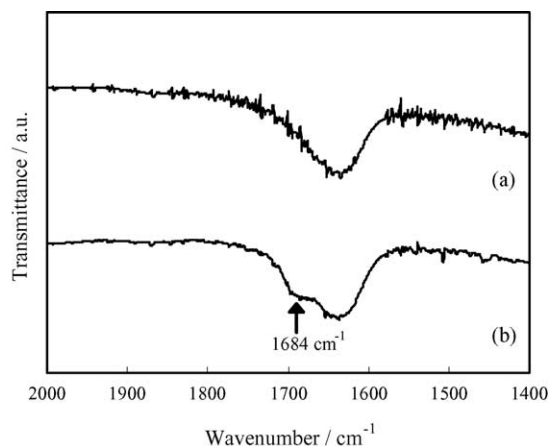

Fig. 5. IR spectra of: (a) Fe-MCM-41-DHT, and (b) Fe-MCM-41-DHT after treatment with cyclohexanone. Fresh Fe-MCM-41-DHT (0.1 g) was treated with cyclohexanone (1.1 equivalent of Fe) in CH_3CN (1 mL) at room temperature, followed by evaporating under vacuum at 40 °C.

3.3. Catalytic behavior of Fe-MCM-41-DHT

Fig. 4 shows the dependency of catalytic activity on the Fe content in the Fe-MCM-41-DHT. With increasing Fe content to 1.1%, the yield of **2** increased, and further increase in the Fe content resulted in a slight decrease in the yield of **2**. This decrease in the yield of **2** at the higher iron content is probably due to the decrease in the surface area as well as the decrease in Fe dispersion (Table 1). These results indicate that an appropriate iron contents in the DHT sample was 1.1 wt%, which was in good agreement with our previous report [26].

The use of a solid catalyst has an advantage of a simple workup procedure over conventional homogeneous catalysts. After the B–V reaction, the Fe-MCM-41-DHT catalyst was readily recovered from the reaction mixture by simple filtration, and could be reused. Table 6 shows the results of the repeated uses of the catalysts for the B–V reactions of cyclohexanone. Yields of 78% were obtained for the repeated oxidations of cyclohexanone without any discernible loss in activity and selectivity. ICP analysis of either the used Fe-MCM-41-DHT or the liquid after the reac-

Table 6
Repeated uses of the Fe-MCM-41-DHT for B–V oxidation of cyclohexanone[a]

Run	Conversion of cyclohexanone (%)[b]	Yield of ε-caprolactone (%)[b]
1 (fresh)	85	77
2	85	78
3	84	77
4	83	78

[a] Reaction conditions; Fe-MCM-41-DHT (0.2 g, Fe: 0.04 mmol), cyclohexanone (1 mmol), benzaldehyde (3 mmol), acetonitrile (10 mL), O_2 (10 mL min^{-1}), 50 °C, 4 h.
[b] Determined by GC and calculated based on cyclohexanone.

tion confirmed that no leaching of Fe species from the catalyst. On the other hand, the iron content slightly dropped from 1.2 to 0.9 wt% after the B–V reaction of **1** for the TIE sample (Table 4, entry 2). During the oxidation of cyclohexanone at 70 °C, Fe-MCM-41-DHT was removed by filtration at ca. 50% conversion of cyclohexanone, and the reaction was continued by using the filtrate, i.e., in the absence of solid catalyst. As a result, neither further consumption of cyclohexanone nor further formation of ε-caprolactone was observed. These results clearly demonstrate that the B–V reaction occurred on the heterogeneous active Fe sites on the Fe-MCM-41-DHT.

3.4. Reaction mechanism

By in situ IR experiments, Corma et al. [31] observed that carbonyl group was coordinatiously activated in the B–V oxidation of cyclohexanone with H_2O_2: $\nu(CO)$ of coordinated cyclohexanone onto Sn/zeolite-β is 48 cm^{-1} lower than that of free cyclohexanone. It is considered that the reaction on Sn/zeolite-β proceeds through a Criegee adduct of the hydrogen peroxide with the activated ketone. A similar reaction mechanism was also proposed for Sn-exchanged hydrotalcites by Pillai and Sahle-Demessie [32]. Fig. 5 shows the IR spectra of: (a) fresh Fe-MCM-41-DHT and (b) Fe-MCM-41-DHT after treatment with cyclohexanone at room temperature. A signal assigned to $\nu(CO)$ of coordinated cyclohexanone was detected at 1684 cm^{-1} after treatment of the Fe-MCM-41-DHT with cyclohexanone, which is 31 cm^{-1} lower than that of free cyclohexanone. This result suggests that the B–V reaction using the Fe-MCM-41-DHT also proceeded via coordination of carbonyl groups of ketone to Fe^{3+} as Lewis acid sites. Autoxidation of benzaldehyde with molecular oxygen produces perbenzoic acid, which attacks activated ketone to form a Criegee adduct [54,55], followed by protolysis to afford the lactone together with benzoic acid.

4. Conclusion

Iron cations were effectively incorporated up to 1.1 wt% inside the framework of MCM-41 by the direct hydrothermal synthesis. The resulting Fe-MCM-41-DHT had a tetrahedrally coordinated Fe species and showed high catalytic activity for the Baeyer–Villiger oxidation of ketones using molecular oxygen and benzaldehyde. It was found that the Lewis acid sites of the Fe-MCM-41-DHT might play an important role in the B–V reactions, and the catalyst was reusable without any appreciable loss in its activity and selectivity.

Acknowledgement

References

[1] C.T. Kresge, M.E. Leonowicz, W.J. Roth, J.C. Vartuli, J.S. Beck, Nature 359 (1992) 710.
[2] A. Corma, Chem. Rev. 97 (1997) 2373.
[3] P.T. Tanev, M. Chibwe, T.J. Pinnavaia, Nature 368 (1994) 321.
[4] A. Corma, M.T. Navarro, J. Pérez Pariente, J. Chem. Soc., Chem. Commun. (1994) 147.
[5] W. Zhang, M. Fröba, J. Wang, P.T. Tanev, J. Wong, T.J. Pinnavaia, J. Am. Chem. Soc. 118 (1996) 9164.
[6] W. Zhang, J. Wang, P.T. Tanev, T.J. Pinnavaia, Chem. Commun. (1996) 979.
[7] K.A. Koyano, T. Tatsumi, Microporous Mater. 10 (1997) 259.
[8] J. Yu, Z. Feng, L. Xu, M. Li, Q. Xin, Z. Liu, C. Li, Chem. Mater. 13 (2001) 994.
[9] A. Hagen, K. Schueler, F. Roessner, Microporous Mesoporous Mater. 51 (2002) 23.
[10] M. Chatterjee, H. Hayashi, N. Saito, Microporous Mesoporous Mater. 57 (2003) 143.
[11] K. Murata, Y. Liu, M. Inaba, N. Mimura, Catal. Today 91–92 (2004) 39.
[12] O.A. Anunziata, A.R. Beltramone, J. Cussa, Appl. Catal. A 270 (2004) 77.
[13] J.M.R. Gallo, I.S. Paulino, U. Schuchardt, Appl. Catal. A 266 (2004) 223.
[14] K.M. Reddy, I. Moudrakovski, A. Sayari, J. Chem. Soc., Chem. Commun. (1994) 1059.
[15] M. Chatterjee, T. Iwasaki, H. Hayashi, Y. Onodera, T. Ebina, T. Nagase, Chem. Mater. 11 (1999) 1368.
[16] Q. Zhang, Y. Wang, Y. Ohishi, T. Shishido, K. Takehira, J. Catal. 202 (2001) 308.
[17] M.J. Jia, R.X. Valenzuela, P. Amorós, D. Beltrán-Porter, J. EI-Haskouri, M.D. Marcos, V. Cortés Corberán, Catal. Today 91–92 (2004) 43.
[18] F. Farzaneh, E. Zamanifar, C.D. Williams, J. Mol. Catal. A 218 (2004) 203.
[19] N. Ulagappan, C.N.R. Rao, Chem. Commun. (1996) 1047.
[20] T.K. Das, K. Chaudhari, E. Nandanan, A.J. Chandwakdar, A. Sudalai, T. Ravindranathan, S. Sivsanker, Tetrahedron Lett. 38 (1997) 3631.
[21] Y. Ohishi, T. Kawabata, T. Shishido, K. Takaki, Q. Zhang, Y. Wang, K. Takehira, J. Mol. Catal. A 230 (2005) 49.
[22] K. Takehira, Y. Ohishi, T. Shishido, T. Kawabata, K. Takaki, Q. Zhang, Y. Wang, J. Catal. 224 (2004) 404.
[23] Y. Wang, Y. Ohishi, K.T. Shishido, Q. Zhang, W. Yang, Q. Guo, H. Wan, K. Takehira, J. Catal. 220 (2003) 347.
[24] A. Sakthivel, P. Selvam, J. Catal. 211 (2002) 134.
[25] A. Wingen, N. Anastasievič, A. Hollnagel, D. Werner, F. Schüth, J. Catal. 193 (2000) 248.
[26] Y. Wang, Q. Zhang, T. Shishido, K. Takehira, J. Catal. 209 (2002) 186.
[27] S. Velu, L. Wang, M. Okazaki, K. Suzuki, S. Tomura, Microporous Mesoporous Mater. 54 (2002) 113.
[28] G.R. Krow, Org. React. 43 (1993) 251.
[29] G. Strukul, Angew. Chem. Int. Ed. 37 (1998) 1198.
[30] M. Renz, B. Meunier, Eur. J. Org. Chem. (1999) 737.
[31] A. Corma, L.T. Nemeth, M. Renz, S. Valencia, Nature 412 (2001) 423.
[32] U.R. Pillai, E. Sahle-Demessie, J. Mol. Catal. A 191 (2003) 93.
[33] S.-I. Murahashi, Y. Oda, T. Naota, Tetrahedron Lett. 33 (1992) 7557.
[34] K. Kaneda, S. Ueno, T. Imanaka, E. Shimotsuma, Y. Nishiyama, Y. Ishii, J. Org. Chem. 59 (1994) 2915.
[35] K. Kaneda, S. Ueno, T. Imanaka, J. Chem. Soc., Chem. Commun. (1994) 797.
[36] K. Kaneda, S. Ueno, T. Imanaka, J. Mol. Catal. A 102 (1995) 135.
[37] I.C. Chisem, J. Chisem, J.H. Clark, N. J. Chem. (1998) 81.
[38] R. Raja, J.M. Thomas, G. Sankar, Chem. Commun. (1999) 525.
[39] K. Kaneda, S. Haruna, T. Imanaka, K. Kawamoto, J. Chem. Soc., Chem. Commun. (1990) 1467.
[40] B.M. Trost, Science 254 (1991) 1471.
[41] P.T. Anastas, J.C. Warner, Green Chemistry: Theory and Practie, Oxford University Press, 1998.
[42] J.H. Clark, Green Chem. 1 (1999) 1.
[43] N.I. Sax, Dangerous Properties of Industrial Materials, sixth ed, Van Nostrand Reinhold Company Inc., New York, 1984.
[44] P. Ratnasami, R. Kumar, Catal. Today 9 (1991) 329.
[45] D. Dollimore, G.R. Heal, J. Appl. Chem. 14 (1964) 109.
[46] T. Tanaka, H. Yamashita, R. Tsuchitani, T. Funabiki, S. Yoshida, J. Chem. Soc., Faraday Trans. 84 (1988) 2987.
[47] A.B. Bourlineos, M.A. Karakassides, D. Petridis, J. Phys. Chem. 104 (2000) 4375.
[48] P. Selvam, S.E. Dapurkar, S.K. Badamali, M. Murugasan, H. Kuwano, Catal. Today 68 (2001) 69.
[49] B. Echchahed, A. Moen, D. Nicholson, L. Bonneviot, Chem. Mater. 9 (1997) 1716.
[50] Y. Kuang, N. He, J. Wang, P. Xiao, C. Yuan, Z. Lu, Colloids Surf. A 179 (2001) 177.
[51] A. Tuel, I. Arcon, J.M.M. Millet, J. Chem. Soc., Faraday Trans. 94 (1998) 3501.
[52] P. Fejes, I. Kiricsi, K. Lázár, I. Marsi, A. Rockenbauer, L. Korecz, Appl. Catal. A 242 (2003) 63.
[53] C. Bolm, G. Schlingloff, K. Weickhardt, Tetrahedron Lett. 34 (1993) 3405.
[54] M. Renz, T. Blasco, A. Corma, V. Fornés, R. Jensen, L. Nemeth, Chem. Eur. J. 8 (2002) 4708.
[55] A. Brunetta, G. Strukul, Eur. J. Inorg. Chem. (2004) 1030.